UMSHA Press

AJDR
Avicenna Journal of Dental Research

Avicenna J Dent Res. 2025;17(4):211-219. doi:10.34172/ajdr.2271

http://ajdr.umsha.ac.ir

Original Article

Computational Screening of Natural Compounds for Pemphigoid Treatment: Identification of High-Affinity Granzyme B Inhibitors

Negar Sharifinejad[1], Yasamin Barakian[2*], Amir Taherkhani[3*], Tina Mazaheri[4]

[1]Student Research Committee, Qom University of Medical Sciences, Qom, Iran
[2]Department of Oral and Maxillofacial Diseases, School of Dentistry, Qom University of Medical Sciences, Qom, Iran
[3]Research Center for Molecular Medicine, Institute of Cancer, Hamadan University of Medical Sciences, Hamadan, Iran
[4]Department of Oral and Maxillofacial Medicine, School of Dentistry, Hamadan University of Medical Sciences, Hamadan, Iran

Article history:
Received: February 23, 2025
Revised: May 25, 2025
Accepted: May 27, 2025
ePublished: December 30, 2025

***Corresponding authors:**
Yasamin Barakian,
Email: dr.ybarakian@muq.ac.ir

Amir Taherkhani,
Email: amir.007.taherkhani@gmail.com

Abstract

Background: Granzyme B (GzmB), a serine protease released by immune and non-immune cells, exhibits a significant presence in pemphigoid lesions. This enzymatic protein degrades extracellular matrix components, playing a crucial role in disease pathogenesis, thus presenting itself as a promising therapeutic target. This study aimed to identify compounds that can hinder GzmB by conducting computational drug discovery using the molecular docking method.

Methods: To this end, 62 plant-derived compounds encompassing three distinct chemical classes (i.e., flavonoid compounds, cinnamic acid derivatives, and anthraquinones) were assessed for their binding affinities to the GzmB active site through molecular docking simulations using AutoDock 4.0.

Results: The analysis revealed remarkable binding characteristics, with 50 compounds demonstrating inhibition constants at nanomolar concentrations and five compounds achieving picomolar-level inhibition. Furthermore, 21 compounds exhibited binding free energies ($\Delta G_{binding}$) below -10, indicating robust interaction with the GzmB active site. Precisely, the Gibbs free energy of binding for Cynarin was calculated to be -13.13 kcal/mol.

Conclusion: This study identified herbal isolates with a strong affinity for GzmB, showing potential for developing treatments for pemphigoid and other immune diseases.

Keywords: Drug, Granzyme B, Inhibitor, Molecular docking, Pemphigoid

Please cite this article as follows: Sharifinejad N, Barakian Y, Taherkhani A, Mazaheri T. Computational screening of natural compounds for pemphigoid treatment: identification of high-affinity Granzyme B inhibitors. Avicenna J Dent Res. 2025;17(4):211-219. doi:10.34172/ajdr.2271

Background

Immunobullous diseases are a group of cutaneous and mucous diseases that can cause death. These diseases are caused by the binding of pathogenic antibodies to protein targets in the skin and mucus. There is a wide range of immunological disorders with specific morphology, which is the cause of various differences in the structural properties of the target protein in these diseases (1).

Pemphigoid is an immunological disease. Some standard clinical features of its types include blisters and erosions (2). This disease's histopathology and clinical manifestations differ in many aspects, including their autoantigens and the course of the disease. The severity of the disease and its distribution vary from mild cases that involve only the oral mucosa to severe cases that involve the eyes, genital areas, and esophageal mucosa (3). This disease includes several subtypes, including bullous pemphigoid, lichen planus pemphigoid, and the like, the most common of which is bullous pemphigoid (4,5). Its early diagnosis is necessary because the consequences of this disease can be severe, and limited treatment options are available (3,5,6). Proteinases, such as neutrophil elastase, chymase, cathepsin-G, Granzyme (Gzm) B, matrix metalloproteinases, and the like, are the basis of many pathological reactions in pemphigoid and have long been suggested as therapeutic targets for this disease (7).

Gzms are a family of serine proteases that include five types in humans (i.e., GzmA, GzmB, GzmH, GzmK, and GzmM). Gzms, discovered in the granules of cytotoxic T cells and natural killer cells, are traditionally regarded as the key mediators of granule-induced cell death that target cancer or virus-infected cells. After internalization in target cells, GzmB initiates apoptosis through caspase-dependent and/or caspase-independent pathways. GzmB can cleave cell receptors, cell adhesion proteins, cytokines, and essential extracellular matrix proteins, thus affecting

tissue structure and function (8,9). Unlike other proteases, such as neutrophil elastase and matrix metalloproteinases, GzmB has no endogenous extracellular inhibitors. Therefore, this protease maintains its proteolytic activity in the extracellular space. However, it is expressed at a low level or not in healthy and non-inflamed tissues. Unhindered GzmB-mediated proteolytic activity in the extracellular space can degrade extracellular proteins and regulate immune responses during inflammation, thereby contributing to pathogenesis (10). GzmB can play multiple roles in the pathogenesis of pemphigoid owing to its wide variety of substrates in inflammatory conditions. For example, it proteolytically enhances the proinflammatory activity of interleukin (IL)-1α, which is predicted to increase neutrophil accumulation in the lesion through subsequent activation of interleukin-8. In addition, this protein mediates the activity of interleukin-8, secretion of macrophage inflammatory protein-2, local infiltration of neutrophils, and regional activity of neutrophil elastase. It has also been shown that the severity of pemphigoid decreases in the case of genetic deficiency of this protein or the local inhibition of GzmB (11). Hence, GzmB plays a pathological role through the breakdown of hemidesmosome proteins and the spread of inflammation in pemphigoid and can be a suitable therapeutic target for this disease (10).

Given the side effects of current pemphigoid therapies (12) and the need for more targeted treatments, finding natural compounds that inhibit GzmB would be a significant step toward safer, more accessible interventions. Therefore, this study aims to identify compounds that can hinder the GzmB enzyme by performing computational drug discovery using the molecular docking method. Molecular simulation offers a helpful approach to identifying binding sites and comprehending the interaction mechanism between a biomolecule and its ligand. Additionally, it provides an *in silico* means to corroborate experimental interpretations (13,14). It also examines how plant-effective substances bind to the active site of the GzmB enzyme and identifies molecules with a lower energy level that bind to the enzyme. These herbal compounds belong to flavonoids, anthraquinones, and cinnamic acid derivatives. It can be considered a drug candidate and can be further evaluated in future laboratory studies.

Methods

Pre-docking Molecular Preparation

The crystallographic data for Gzm (Protein Data Bank identifier: 1IAU; 2.0 Å resolution) were sourced from the Research Collaboratory for Structural Bioinformatics repository (15,16), accessible at https://www.rcsb.org. The obtained file detailed a monomeric protein encompassing 227 amino acids. A state of optimal stability for the enzyme was acquired by refinement through energy minimization, employing the Swiss-PdbViewer, version 4.1.0 (available at https://spdbv.unil.ch). Critical amino acids within the enzyme's active site are histidine 57, aspartate 102, aspartate 194, lysine 192, glycine 193, serine 195, serine 214, asparagine 218, and arginine 226 (17). A set of 62 natural compounds was curated to evaluate inhibitory interactions against 1IAU. This ensemble comprised 36 flavonoids, 14 anthraquinones, and 12 cinnamic acids. The inclusion criterion for all compounds was that they had to be natural (not synthetic). Furthermore, these compounds were also used in previous docking analyses. The energy minimization of these drug candidates was executed using the HyperChem software Version 8.0.10 (18). For computational analysis, the 1IAU protein and candidate molecules were prepared as PDBQT files, incorporating Kollmann charges and polar hydrogens to the macromolecule and imparting conformational flexibility and local charges to the ligands. The calculations were facilitated via MGL tools.

Molecular Docking

For docking analyses, the employed system consisted of a Windows-operated computer equipped with an Intel Core i7 processor and 16 GB of RAM running on a 64-bit operating architecture. The assessment of the binding free energy ($\Delta G_{binding}$) expressed in kcal/mol was performed through AutoDock 4.0 software using a semi-flexible docking approach (19). The defined parameters for the grid box within which the docking was conducted were 50 units on the X-axis, 54 units on the Y-axis, and 48 units on the Z-axis, with respective centers at coordinates 13.382, 37.317, and 71.742, and a grid spacing of 0.375 Å. Each molecular entity was subjected to the generation of 100 potential models via the Lamarckian genetic algorithm, aimed at appraising the binding biases of the phytochemicals under study within the 1IAU enzyme's active site.

Conformations resulting from the docking simulation were grouped based on a root mean square deviation tolerance of 2.0 Å. Within the most populated cluster, the conformation exhibiting the most formidable $\Delta G_{binding}$ value was taken forward for detailed examination.

Interaction Mode Analysis

The visualization and scrutiny of the interaction patterns were facilitated through the Discovery Studio Visualizer tool, providing an informative depiction of molecular engagements. These visualizations are integral to discerning the stabilizing interactions and informing subsequent experimental validation steps, thereby enhancing the comprehension of the molecular docking profiles and the efficiency of potential inhibitors.

Results

Binding Energies

The current investigation identified compounds exhibiting a $\Delta G_{binding}$ value of < -10 kcal/mol within the 1IAU catalytic cleft as the most potent Gzm inhibitors. Among flavonoids, kaempferol 3-rutinoside-

7-sophoroside, vicenin-2, sophoraflavanone G, amentoflavone, kaempferol 7-O-glucoside, orientin, quercetin-3-rhamnoside, isoquercitrin, apigenin-7-glucoside, kaempferol 3-rutinoside-4'-glucoside, vitexin, and dihydroquercetin demonstrated notable inhibitory effects. In anthraquinones, pulmatin (chrysophanol-8-0-glucoside), aloe emodin 8-glucoside, emodin-8-glucoside, knipholone, sennidin B, and sennidin A emerged as the most potent 1IAU inhibitors. Similarly, cynarin, caffeic acid 3-glucoside, and chlorogenic acid were identified as top-ranked inhibitors from cinnamic acid derivatives.

Table 1 lists the $\Delta G_{binding}$ values between all the tested compounds in this study and the 1IAU catalytic cleft. Energy types between the top-ranked compound and the 1IAU active site are presented in Table 2. In addition, Figure 1 compares the $\Delta G_{binding}$ values between the highest-ranked herbal ligands and the 1IAU active site.

Table 1. Gibbs Free Binding Energy and Inhibition Constants of Anthraquinones, Flavonoids, and Cinnamic Acids With Granzyme B

PubChem ID	Ligand Name	Binding Energy (kcal/mol)	Ki
Anthraquinones			
442731	Pulmatin (chrysophanol-8-*0*-glucoside)	-13.04	274.16 pM
126456371	Aloe emodin 8-glucoside	-12.95	319.62 pM
99649	Emodin-8-glucoside	-12.63	550.36 pM
442753	Knipholone	-11.64	2.94 nM
10459879	Sennidin B	-11.55	3.44 nM
92826	Sennidin A	-11.06	7.82 nM
101286218	Rhodoptilometrin	-9.62	88.68 nM
6683	Purpurin	-9.5	107.92 nM
361510	Emodic acid	-9.32	148.43 nM
3083575	Obtusifolin	-9.03	240.29 nM
2948	Damnacanthal	-8.57	518.63 nM
2950	Danthron	-8.53	558.75 nM
160712	Nordamnacanthal	-8.51	576.44 nM
10207	Aloe-emodin	-8.34	775.15 nM
Flavonoids			
44258853	Kaempferol 3-rutinoside-7-sophoroside	-13.09	254.73 pM
442664	Vicenin-2	-12.21	1.11 nM
72936	Sophoraflavanone G	-11.74	2.47 nM
5281600	Amentoflavone	-11.62	3.04 nM
10095180	Kaempferol 7-O-glucoside	-11.31	5.10 nM
5281675	Orientin	-10.87	10.73 nM
5353915	Quercetin-3-rhamnoside	-10.72	13.65 nM
5280804	Isoquercitrin	-10.71	14.02 nM
5280704	Apigenin-7-glucoside	-10.54	18.95 nM
44258844	Kaempferol 3-rutinoside-4'-glucoside	-10.54	18.71 nM
5280441	Vitexin	-10.44	22.07 nM
471	Dihydroquercetin	-10.1	39.83 nM
639665	Xanthohumol	-9.82	63.67 nM
5280681	3-O-Methylquercetin	-9.48	111.84 nM
72281	Hesperetin	-9.42	123.56 nM
5280445	Luteolin	-9.24	168.07 nM
5316673	Afzelin	-9.19	184.07 nM
5318998	Licochalcone A	-9.14	198.19 nM
72277	Epigallocatechin	-9.04	237.84 nM
5280443	Apigenin	-8.94	280.61 nM
5281670	Morin	-8.94	278.71 nM
5280343	Quercetin	-8.81	345.56 nM
5281612	Diosmetin	-8.77	372.05 nM
5281654	Isorhamnetin	-8.66	448.02 nM
5317435	Fustin	-8.63	468.90 nM
5281672	Myricetin	-8.55	542.39 nM
5281614	Fisetin	-8.51	577.40 nM
5281607	Chrysin	-8.48	610.84 nM
1203	Epicatechin	-8.45	641.89 nM
5280637	Cynaroside	-8.45	635.63 nM
14309735	Xanthogalenol	-8.36	739.74 nM
629440	Hemileiocarpin	-8.29	831.22 nM
5280544	Herbacetin	-8.11	1.13 uM
124052	Glabridin	-7.83	1.82 uM
10680	Flavone	-7.71	2.25 uM
443639	Epiafzelechin	-7.43	3.58 uM
Cinnamic Acids			
6124212	Cynarin	-13.13	239.01 pM
5281759	Caffeic acid 3-glucoside	-11.7	2.65 nM
1794427	Chlorogenic acid	-10.11	38.88 nM
5281792	Rosmarinic acid	-9.89	56.73 nM
689043	Caffeic acid	-8.56	531.08 nM
637540	O-Coumaric acid	-8.55	537.44 nM
5281787	Caffeic acid phenethyl ester	-8.46	627.79 nM
637775	Sinapinic acid	-8.32	790.28 nM
5372945	N-p-Coumaroyltyramine	-8.21	960.33 nM
445858	Ferulic acid	-8.03	1.29 uM
637542	P-Coumaric acid	-7.26	4.78 uM
444539	Cinnamic acid	-6.95	8.05 uM

Note. Ki: Inhibition constant.

Interaction Mode Analysis

The Discovery Studio Visualizer revealed various interaction patterns between high-affinity 1IAU inhibitors and residues at the enzyme's catalytic site. Among the studied compounds, representatives of three chemical classes demonstrated exceptional hydrogen bonding capabilities with 1IAU: kaempferol 3-rutinoside-4'-glucoside (flavonoid), aloe-emodin 8-glucoside (anthraquinone), and cynarin (cinnamic acid derivative). Specifically, kaempferol 3-rutinoside-4'-glucoside formed

Table 2. Contributing Binding Energies (kcal/mol) of Top-Ranked Compounds With Granzyme B Active Site

A. Anthraquinones					
Ligand Name	**Intermolecular Energy**	**Total Internal Energy**	**Torsional Free Energy**	**Unbound System Energy**	**Estimated Free Binding Energy**
Pulmatin (chrysophanol-8-*O*-glucoside)	-11.07	-5.36	2.39	-0.99	-13.04
Aloe emodin 8-glucoside	-11.53	-5.39	2.98	-0.99	-12.95
Emodin-8-glucoside	-10.95	-5.36	2.68	-0.99	-12.63
Knipholone	-12.3	-2.72	2.09	-1.28	-11.64
Sennidin B	-11.17	-5.3	2.68	-2.24	-11.55
Sennidin A	-12.05	-3.42	2.68	-1.73	-11.06
B. Flavonoids					
Ligand Name	**Intermolecular Energy (kcal/mol)**	**Total Internal Energy (kcal/mol)**	**Torsional Free Energy (kcal/mol)**	**Unbound System Energy (kcal/mol)**	**Estimated Free Binding Energy (kcal/mol)**
Apigenin-7-glucoside	-11.09	-3.48	2.98	-1.05	-10.54
Orientin	-10.35	-5.03	3.28	-1.22	-10.87
Vitexin	-10.34	-4.21	2.98	-1.12	-10.44
Isoquercitrin	-9.88	-5.93	3.58	-1.52	-10.71
Quercetin-3-rhamnoside	-11	-4.13	2.98	-1.42	-10.73
Vicenin-2	-11.29	-8.17	4.77	-2.47	-12.21
Amentoflavone	-9.52	-6.16	2.68	-1.38	-11.62
Kaempferol 7-O-glucoside	-11.55	-0.19	0.3	-0.13	-11.31
Kaempferol 3-rutinoside-7-sophoroside	-12.75	-4.42	2.68	-1.39	-13.09
Kaempferol 3-rutinoside-4'-glucoside	-10.99	-3.17	2.09	-1.53	-10.54
Dihydroquercetin	-10.1	0	0	0	-10.1
Sophoraflavanone G	-11.97	-2.02	1.19	-1.05	-11.74
C. Cinnamic Acids					
Ligand Name	**Intermolecular Energy (kcal/mol)**	**Total Internal Energy (kcal/mol)**	**Torsional Free Energy (kcal/mol)**	**Unbound System Energy (kcal/mol)**	**Estimated Free Binding Energy (kcal/mol)**
Cynarin	-13.26	-6.53	5.37	-1.29	-13.13
Caffeic acid 3-glucoside	-12.28	-3.95	3.58	-0.94	-11.7
Chlorogenic acid	-10.41	-4.48	3.58	-1.21	-10.11

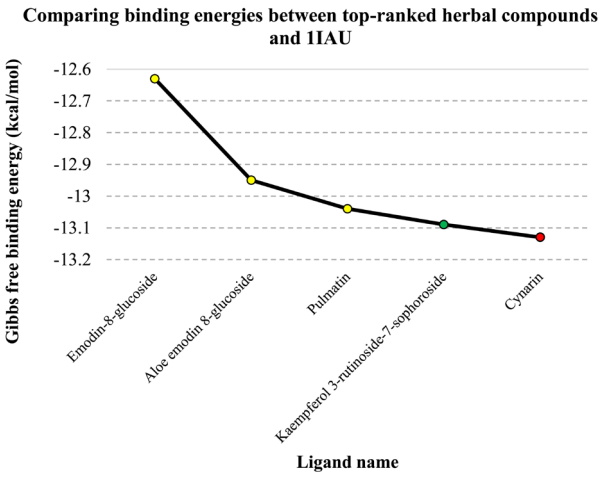

Figure 1. A Comparative Analysis of the Binding Energies ($\Delta G_{binding}$, kcal/mol) Between Top-Performing Compounds and the Granzyme B Active Site. *Note*. All ligands demonstrated potent inhibition at the picomolar scale. The graph plots ligand names (X-axis) against their respective $\Delta G_{binding}$ values (Y-axis). Ligand classes are distinguished by color: Cinnamic acid (red), flavonoid (green), and anthraquinones (yellow)

nine hydrogen bonds, and aloe-emodin 8-glucoside established eight hydrogen bonds. In addition, cynarin generated seven hydrogen bonds with residues in the 1IAU binding pocket (Table 3). The spatial arrangements and binding configurations of the most effective inhibitors from each structural class within the 1IAU structure are illustrated in 2D and 3D representations in Figure 2.

Discussion

The GzmB enzyme is integral to numerous biological processes, and its elevated activity has been linked to various pathological conditions (20), including bullous and erosive pemphigoid. Consequently, suppressing GzmB enzymatic activity represents a promising therapeutic approach for pemphigoid treatment (21). In contrast to conventional drug development approaches, which require substantial time and financial investment (22), computational methodologies enable scientists to obtain crucial insights regarding drug candidates' pharmacodynamics, pharmacokinetics, and toxicological profiles (23).

In this study, a virtual screening technique was employed through AutoDock software to evaluate 62 small molecules, aiming to identify compounds exhibiting strong binding affinity to the GzmB. According to the

Table 3. Analysis of Interaction Types Between Top-Ranked Herbal Isolates and Granzyme B Catalytic Domain

Anthraquinones			
Ligand Name	**Hydrogen Bond (Distance Å)**	**Hydrophobic Interaction (Distance Å)**	**Electrostatic Interaction (Distance Å)**
Pulmatin	Gly216(3.07); Gly193(3.21, 3.72); Ser195(3.21, 4.55)	Lys192(5.29, 4.60, 4.05); Val213(5.30)	Lys192(5.29, 4.60)
Aloe emodin 8-glucoside	Gly216(3.04); Ser190(3.74); Arg226(3.85); Gly193(3.58); Ser195(4.53, 4.63, 3.33, 3.44)	Lys192(5.33, 4.64, 4.09)	Lys192(5.33, 4.64)
Emodin-8-glucoside	Gly216(3.05); Gly193(3.70); Ser195 (3.19, 4.55); Arg41(7.28)	Val213(5.24); His57(6.37); Lys192(4.06, 4.65)	NA
Knipholone	Gly193(3.68); Ser195(4.38, 3.20); Gly216(3.13)	Lys192(4.80, 4.80, 4.29); Tyr174(4.77); Arg217 (3.78)	Lys192(4.80, 4.80)
Sennidin A	Gly193(3.61); Ser195(3.11); Gly216(3.12, 3.08)	Lys192(4.72); His57(6.24); Lys40(6.51)	Lys192(4.72)
Sennidin B	Asn218(3.96); Gly216(2.98); Ser195(2.79); Gly193(3.51), Asp194(4.45)	His57(6.20); Lys40(6.51); Lys192(4.64); Phe99(6.41)	Lys40(6.51); Lys192(4.64)
Flavonoids			
Ligand Name	**Hydrogen Bond (Distance Å)**	**Hydrophobic Interaction (Distance Å)**	**Electrostatic Interaction (Distance Å)**
Apigenin-7-glucoside	Arg226(4.84); Gly216(3.81); Ser195(4.17, 3.77)	Lys192(4.41, 3.99)	Lys192(4.41)
Orientin	Gly193(3.34); Ser195(2.59, 4.65, 3.49)	Lys192(4.08,5.82); Lys40(4.38); His57(6.91)	NA
Vitexin	Ser195(3.31); Gly193(2.82); Gly216(2.87)	His57(5.79); Lys192(4.48, 5.79); Lys40(5.22)	Lys40(5.22)
Isoquercitrin	Gly193(3.69) ;Lys192(3.55); Arg226(3.56); Ser195(3.32, 4.25, 3.68); His57(3.89)	Lys192(4.31, 5.31); His57(5.49)	NA
Quercetin-3-rhamnoside	Gly216(3.56); Ser195(2.98, 4.66); Ser214(4.15,3.47); Arg226(4.16)		NA
Vicenin-2	Ser190(3.13); Lys192(4.75); Gly216(2.32, 2.83); Lys40(4.19)	Val213 (6.54); Lys192(4.17, 4.75, 3.89, 5.22); His57(5.83)	NA
Amentoflavone	Ser214(2.88); Arg226(4.69); Ser195(3.88, 4.81)	His57(4.98, 6.30); Phe99(5.84); Val213(6.23); Lys40(5.69); Lys192(5.40, 4.04, 4.38); Val213(6.23)	NA
Kaempferol 7-O-glucoside	Gln143(4.62); Ser195(3.15) ;Gly193(3.29);Asp194(4.47)	His57(6.59)	Lys192(4.44)
Kaempferol 3-rutinoside-7-sophoroside	Ser38(4.16, 3.21); Arg226(4.19); Ser190(4.13);Lys192(4.75)	Phe99(5.69); Tyr215(3.96); Lys192(4.33)	NA
Kaempferol 3-rutinoside-4'-glucoside	Lys192(4.91, 4.64, 4.60); Arg41(3.69); His57(4.27); Gly193(4.14); GY216(3.86, 3.43); Gln143(3.42)	Arg41(4.69, 6.63); Lys192(4.64, 4.60)	NA
Dihydroquercetin	Gly216(4.24, 3.77); Gly193(3.73); Ser195(3.46, 3.77)	Lys192(4.52)	NA
Sophoraflavanone G	Arg226(4.43); Ser195(4.65, 3.39); Gly193(3.34); Asp194(4.11)	Lys192(3.83); His57(6.07 ,6.48, 5.05, 4.05); Tyr215(4.71); Phe99(6.34, 5.65, 7.87, 3.87)	Lys40(7.46)
Cinnamic Acids			
Ligand Name	**Hydrogen Bond (Distance Å)**	**Hydrophobic Interaction (Distance Å)**	**Electrostatic Interaction (Distance Å)**
Cynarin	Lys192(3.65); Asp194(4.23); Ser190(4.14); Ser195(3.01, 3.65, 4.03, 2.64)	Lys192(4.67, 5.75); Ser190(6.96); Lys40(4.65); His57(6.22)	Lys40(4.65)
Caffeic acid 3-glucoside	Gly193(3.34); Ser195(2.59, 4.65);	Lys192(4.08, 5.82); Lys40(4.38); His57(6.91)	NA
Rosmarinic acid	Arg226(3.56); Ser195(3.25); Asp194(4.07); Gly193(3.14)	Lys192(4.06, 4.50); Lys40(6.45)	Arg226(6.20);Lys40(6.45);
Chlorogenic acid	Ser190(3.91); Ser195(4.07, 3.54)	Lys192(4.63)	NA

Note. Critical amino acids within the enzyme's active site are marked in bold. NA: Not available.

results, 21 compounds demonstrated high binding affinity to the GzmB active site, characterized by notable inhibition constants and $\Delta G_{binding}$ values. The superior performance of these compounds can be attributed to their distinctive structural characteristics and capacity to establish hydrogen, ionic, and hydrophobic interactions with the protein's amino acid residues (24). Cynarin displayed the most potent inhibitory activity, with $\Delta G_{binding}$ and Ki values of -13.13 kcal/mol and 239.01 pm, respectively.

Chen et al (25) demonstrated that dihydroquercetin administration led to decreased levels of multiple inflammatory mediators in damaged hepatic tissue, including proinflammatory cytokines (tumor necrosis factor-α, interferon-γ, IL-2, IL-4, and IL-10), chemokine

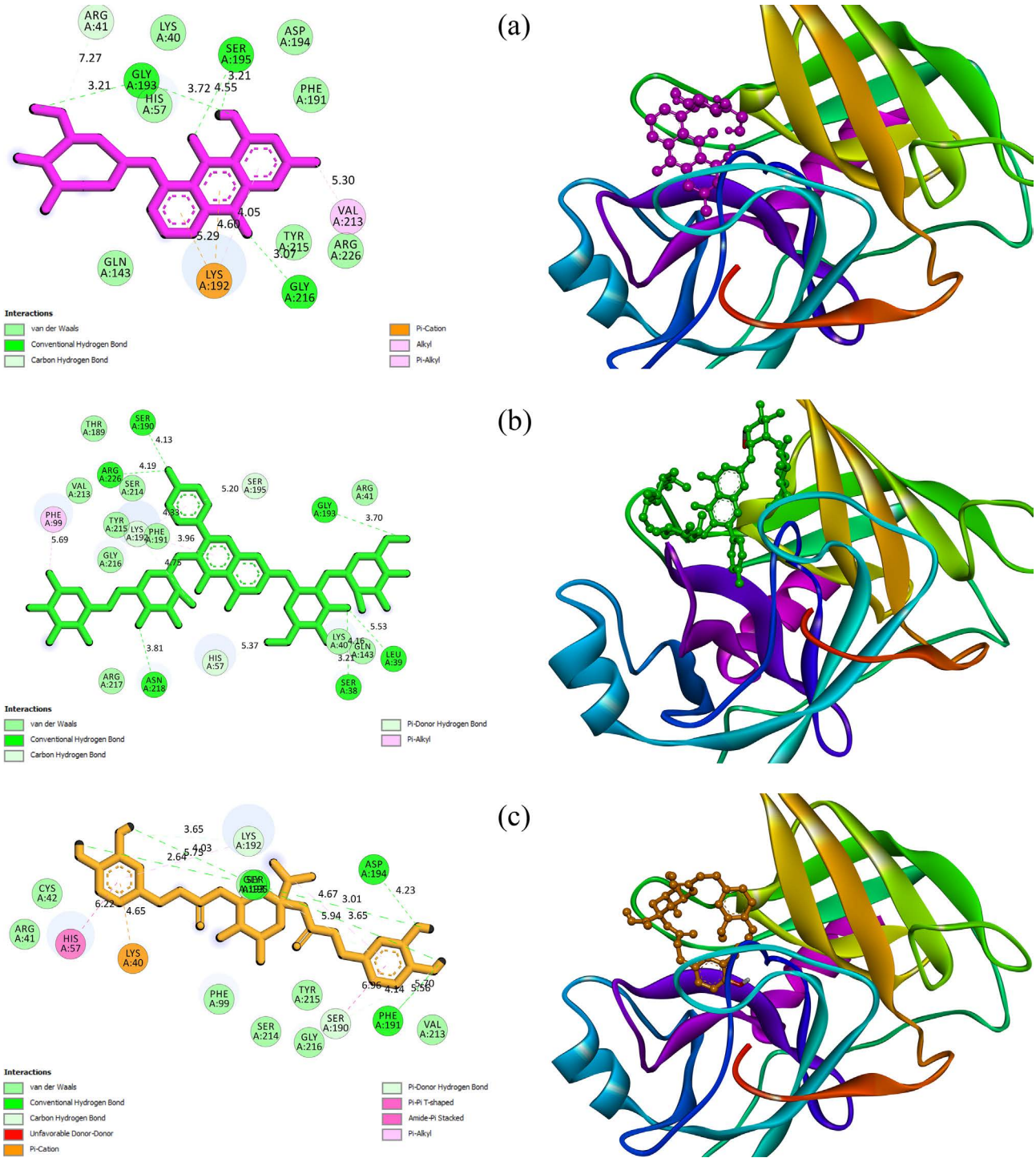

Figure 2. Ligand-Protein Interactions Visualization: 2D and 3D Representations of **(a)** Pulmatin, **(b)** Kaempferol 3-Rutinoside-7-Sophoroside, and **(c)** Cynarin Within the Granzyme B Active Site

osteopontin, apoptotic factors (Fas and FasL), cell differentiation transcription factors (T-bet and GATA-3), perforin, nitric oxide synthase, and GzmB. Furthermore, quercetin showed therapeutic potential in managing rheumatoid arthritis, an autoimmune condition. The present findings revealed substantial GzmB binding affinities for both quercetin and quercetin-3-rhamnoside, with binding energy values at the enzyme's active site of -8.81 kcal/mol and -10.72 kcal/mol, respectively.

Oswald et al (26) examined the therapeutic efficacy of luteolin in rabbit models of pemphigoid, documenting a reduction in both respiratory episodes and autoantibody-induced epidermal detachment. According to the present study, luteolin represented a strong binding affinity to the GzmB active site ($\Delta G_{binding}$ = -9.24 kcal/mol), suggesting that the therapeutic benefit of luteolin in pemphigoid treatment may be partially attributed to its ability to suppress GzmB activity.

Type 1 diabetes mellitus is an autoimmune disorder characterized by CD4+and CD8+cell-mediated destruction of pancreatic β-cells through the secretion of cytokines, perforin, and Gzm, resulting in diminished

insulin production. Previous research has shown that a 10-day apigenin treatment regimen in the murine models of type 1 diabetes facilitated normal insulin production and reduced hyperglycemia (27). Additionally, apigenin exhibited therapeutic potential across various autoimmune disorders, including rheumatoid arthritis (28), systemic lupus erythematosus, multiple sclerosis (29), myocarditis (30), and ulcerative colitis (31). Our findings confirmed a considerable binding affinity of apigenin to the GzmB catalytic site, with a molecular binding energy of -9.94 kcal/mol.

Based on the findings of the study by Chen et al (32), anthraquinones extracted from *Rhei Radix et Rhizoma* demonstrated therapeutic efficacy across numerous autoimmune conditions, including atherosclerosis, multiple sclerosis, gout, rheumatoid arthritis, ulcerative colitis, type 1 diabetes mellitus, immunoglobulin A nephropathy, and autoimmune thyroiditis. The present study revealed notable results for anthraquinone compounds, with the pulmatin ligand exhibiting auspicious outcomes.

Sorrenti et al (33) found that caffeic acid phenethyl ester, a cinnamic acid derivative, had therapeutic potential in treating type 1 diabetes mellitus. Our findings indicated that caffeic acid 3-glucoside exhibited exceptional binding affinity to GzmB, with a $\Delta G_{binding}$ value of -12.28 kcal/mol.

Wang et al (34) investigated novel rheumatoid arthritis targets, specifically focusing on identifying GzmB inhibitors through molecular docking. This computational approach successfully screened natural compounds, leading to the identification of ZINC000004557101, ZINC000012495776, and ZINC000038143593 as potent GzmB binders. Subsequent toxicity analysis and molecular dynamics simulations further validated these compounds, particularly ZINC000004557101, as promising therapeutic candidates, demonstrating the efficiency of this computational drug discovery pipeline.

The current computational study identified potent GzmB inhibitory activity among the tested compounds, with 21 molecules representing particularly robust effects. While this research utilized advanced software and bioinformatics methodologies, experimental validation studies are essential to confirm these *in silico* findings. Given our focus on plant-derived compounds as ligands, we recommend expanding future investigations to examine the inhibitory potential of natural compounds from non-herbal sources.

Several limitations should be considered when interpreting the findings of this study. While molecular docking simulations provide valuable insights into potential binding interactions, they represent idealized conditions that may not fully reflect the complex biological environment. This study focused solely on computational analysis without experimental validation through in vitro or in vivo studies, which would be necessary to confirm the predicted inhibitory effects. Furthermore, while the binding energies and interaction patterns were thoroughly analyzed, the present study did not evaluate the compounds' kinetics or their ability to maintain the sustained inhibition of GzmB under dynamic conditions.

Conclusion

This comprehensive computational study identified several promising plant-derived compounds as potential GzmB inhibitors, with powerful results across flavonoids, anthraquinones, and cinnamic acid derivatives. Among the tested compounds, pulmatin, aloe emodin 8-glucoside, and emodin-8-glucoside (anthraquinones), kaempferol 3-rutinoside-7-sophoroside (flavonoid), and cynarin (cinnamic acid) emerged as the most potent GzmB inhibitors, exhibiting picomolar Ki values. These five herbal compounds are strong candidates for further experimental analysis and potential use in pemphigoid treatment. Notably, compounds such as cynarin demonstrated exceptional binding free energy (-13.13 kcal/mol), while representatives from each chemical class exhibited substantial hydrogen bonding capabilities with the GzmB active site. These findings establish a strong foundation for developing natural compound-based therapeutics for pemphigoid and other GzmB-mediated conditions. The identified compounds, particularly those with binding energies below -10 kcal/mol, warrant further investigation to advance their development as therapeutic agents through experimental validation. This study represents a significant step forward in identifying natural GzmB inhibitors and opens new avenues for treating immune-related diseases.

Acknowledgments

We thank the Student Research Committee and Department of Oral and Maxillofacial Medicine, Qom University of Medical Sciences, Qom, and the Research Center for Molecular Medicine, Institute of Cancer, Hamadan University of Medical Sciences, Hamadan, Iran, for their support.

Authors' Contribution

Conceptualization: Amir Taherkhani, Negar Sharifinejad, Yasamin Barakian.
Data curation: Amir Taherkhani, Negar Sharifinejad, Yasamin Barakian.
Formal analysis: Amir Taherkhani, Negar Sharifinejad, Yasamin Barakian.
Investigation: Amir Taherkhani, Negar Sharifinejad, Yasamin Barakian.
Methodology: Amir Taherkhani, Negar Sharifinejad, Yasamin Barakian, Tina Mazaheri.
Project administration: Amir Taherkhani, Yasamin Barakian.
Resources: Amir Taherkhani, Negar Sharifinejad, Yasamin Barakian.
Software: Amir Taherkhani, Negar Sharifinejad, Tina Mazaheri.
Supervision: Amir Taherkhani, Yasamin Barakian.
Validation: Amir Taherkhani, Negar Sharifinejad, Yasamin Barakian.
Visualization: Amir Taherkhani, Negar Sharifinejad, Yasamin Barakian.
Writing-original draft: Negar Sharifinejad.
Writing-review & editing: Amir Taherkhani.

Competing Interests

The authors declare that they have no competing interests.

Consent for Publication
Not applicable.

Data Availability Statement
The datasets used and/or analyzed during the current study are available from the corresponding author upon reasonable request.

Ethical Approval
The present study has been confirmed by the Ethics Committee of Qom University of Medical Sciences, Qom, Iran (IR.MUQ.REC.1400.220.).

Funding
This research received no specific grant from any funding agency in the public, commercial, or not-for-profit sectors.

References
1. Persson MS, Begum N, Grainge MJ, Harman KE, Grindlay D, Gran S. The global incidence of bullous pemphigoid: a systematic review and meta-analysis. Br J Dermatol. 2022;186(3):414-25. doi: 10.1111/bjd.20743.
2. Schmidt E, Zillikens D. Pemphigoid diseases. Lancet. 2013;381(9863):320-32.doi:10.1016/s0140-6736(12)61140-4.
3. Xu HH, Werth VP, Parisi E, Sollecito TP. Mucous membrane pemphigoid. Dent Clin North Am. 2013;57(4):611-30. doi: 10.1016/j.cden.2013.07.003.
4. Hofmann SC, Juratli HA, Eming R. Bullous autoimmune dermatoses. J Dtsch Dermatol Ges. 2018;16(11):1339-58. doi: 10.1111/ddg.13688.
5. Scully C, Lo Muzio L. Oral mucosal diseases: mucous membrane pemphigoid. Br J Oral Maxillofac Surg. 2008;46(5):358-66. doi: 10.1016/j.bjoms.2007.07.200.
6. Chan LS. Ocular and oral mucous membrane pemphigoid (cicatricial pemphigoid). Clin Dermatol. 2012;30(1):34-7. doi: 10.1016/j.clindermatol.2011.03.007.
7. Hiroyasu S, Turner CT, Richardson KC, Granville DJ. Proteases in pemphigoid diseases. Front Immunol. 2019;10:1454. doi: 10.3389/fimmu.2019.01454.
8. Vahedi F, Fraleigh N, Vlasschaert C, McElhaney J, Hanifi-Moghaddam P. Human granzymes: related but far apart. Med Hypotheses. 2014;83(6):688-93. doi: 10.1016/j.mehy.2014.09.019.
9. Russo V, Klein T, Lim DJ, Solis N, Machado Y, Hiroyasu S, et al. Granzyme B is elevated in autoimmune blistering diseases and cleaves key anchoring proteins of the dermal-epidermal junction. Sci Rep. 2018;8(1):9690. doi: 10.1038/s41598-018-28070-0.
10. Hiroyasu S, Zeglinski MR, Zhao H, Pawluk MA, Turner CT, Kasprick A, et al. Granzyme B inhibition reduces disease severity in autoimmune blistering diseases. Nat Commun. 2021;12(1):302. doi: 10.1038/s41467-020-20604-3.
11. Dou D. Mammalian and Viral Protease Inhibitors [dissertation]. Wichita State University; 2010.
12. Singh S, Kirtschig G, Anchan VN, Chi CC, Taghipour K, Boyle RJ, et al. Interventions for bullous pemphigoid. Cochrane Database Syst Rev. 2023;8(8):CD002292. doi: 10.1002/14651858.CD002292.pub4.
13. Bahmani A, Tanzadehpanah H, Hosseinpour Moghadam N, Saidijam M. Introducing a pyrazolopyrimidine as a multi-tyrosine kinase inhibitor, using multi-QSAR and docking methods. Mol Divers. 2021;25(2):949-65. doi: 10.1007/s11030-020-10080-8.
14. Tanzadehpanah H, Bahmani A, Hosseinpour Moghadam N, Gholami H, Mahaki H, Farmany A, et al. Synthesis, anticancer activity, and β-lactoglobulin binding interactions of multitargeted kinase inhibitor sorafenib tosylate (SORt) using spectroscopic and molecular modelling approaches. Luminescence. 2021;36(1):117-28. doi: 10.1002/bio.3929.
15. Burley SK, Bhikadiya C, Bi C, Bittrich S, Chen L, Crichlow GV, et al. RCSB Protein Data Bank: powerful new tools for exploring 3D structures of biological macromolecules for basic and applied research and education in fundamental biology, biomedicine, biotechnology, bioengineering and energy sciences. Nucleic Acids Res. 2021;49(D1):D437-51. doi: 10.1093/nar/gkaa1038.
16. Chen CC, Herzberg O. Inhibition of beta-lactamase by clavulanate. Trapped intermediates in cryocrystallographic studies. J Mol Biol. 1992;224(4):1103-13. doi: 10.1016/0022-2836(92)90472-v.
17. Rotonda J, Garcia-Calvo M, Bull HG, Geissler WM, McKeever BM, Willoughby CA, et al. The three-dimensional structure of human granzyme B compared to caspase-3, key mediators of cell death with cleavage specificity for aspartic acid in P1. Chem Biol. 2001;8(4):357-68. doi: 10.1016/s1074-5521(01)00018-7.
18. Froimowitz M. HyperChem: a software package for computational chemistry and molecular modeling. Biotechniques. 1993;14(6):1010-3.
19. Trott O, Olson AJ. AutoDock Vina: improving the speed and accuracy of docking with a new scoring function, efficient optimization, and multithreading. J Comput Chem. 2010;31(2):455-61. doi: 10.1002/jcc.21334.
20. Trimarchi M, Bellini C, Fabiano B, Gerevini S, Bussi M. Multiple mucosal involvement in cicatricial pemphigoid. Acta Otorhinolaryngol Ital. 2009;29(4):222-5.
21. Chen HC, Wang CW, Toh WH, Lee HE, Chung WH, Chen CB. Advancing treatment in bullous pemphigoid: a comprehensive review of novel therapeutic targets and approaches. Clin Rev Allergy Immunol. 2023;65(3):331-53. doi: 10.1007/s12016-023-08973-1.
22. Hillisch A, Hilgenfeld R. Modern Methods of Drug Discovery. Springer Science & Business Media; 2002.
23. Chawla R, Rani V, Mishra M, Kumar K. Computer simulation and modeling in pharmacokinetics and pharmacodynamics. In: Saharan VA, ed. Computer Aided Pharmaceutics and Drug Delivery: An Application Guide for Students and Researchers of Pharmaceutical Sciences. Singapore: Springer; 2022. p. 217-54. doi: 10.1007/978-981-16-5180-9_8.
24. Sarkhel S, Desiraju GR. N-H...O, O-H...O, and C-H...O hydrogen bonds in protein-ligand complexes: strong and weak interactions in molecular recognition. Proteins. 2004;54(2):247-59. doi: 10.1002/prot.10567.
25. Chen J, Sun X, Xia T, Mao Q, Zhong L. Pretreatment with dihydroquercetin, a dietary flavonoid, protected against concanavalin A-induced immunological hepatic injury in mice and TNF-α/ActD-induced apoptosis in HepG2 cells. Food Funct. 2018;9(4):2341-52. doi: 10.1039/c7fo01073g.
26. Oswald E, Sesarman A, Franzke CW, Wölfle U, Bruckner-Tuderman L, Jakob T, et al. The flavonoid luteolin inhibits Fcγ-dependent respiratory burst in granulocytes, but not skin blistering in a new model of pemphigoid in adult mice. PLoS One. 2012;7(2):e31066. doi: 10.1371/journal.pone.0031066.
27. Kasiri N, Rahmati M, Ahmadi L, Eskandari N. The significant impact of apigenin on different aspects of autoimmune disease. Inflammopharmacology. 2018;26(6):1359-73. doi: 10.1007/s10787-018-0531-8.
28. Rudan I, Sidhu S, Papana A, Meng SJ, Xin-Wei Y, Wang W, et al. Prevalence of rheumatoid arthritis in low- and middle-income countries: a systematic review and analysis. J Glob Health. 2015;5(1):010409. doi: 10.7189/jogh.05.010409.
29. Belbasis L, Bellou V, Evangelou E, Ioannidis JP, Tzoulaki I. Environmental risk factors and multiple sclerosis: an umbrella review of systematic reviews and meta-analyses. Lancet Neurol. 2015;14(3):263-73. doi: 10.1016/s1474-4422(14)70267-4.
30. Liu X, Zhang X, Ye L, Yuan H. Protective mechanisms of

berberine against experimental autoimmune myocarditis in a rat model. Biomed Pharmacother. 2016;79:222-30. doi: 10.1016/j.biopha.2016.02.015.
31. Sadraei H, Asghari G, Khanabadi M, Minaiyan M. Anti-inflammatory effect of apigenin and hydroalcoholic extract of *Dracocephalum kotschyi* on acetic acid-induced colitis in rats. Res Pharm Sci. 2017;12(4):322-9. doi: 10.4103/1735-5362.212050.
32. Chen QY, Fu CM, Luo RF, Lin MS, Liao W, Gao F. [Research progress of effect of Rhei Radix et Rhizoma and its anthraquinone in treatment of autoimmune diseases]. Zhongguo Zhong Yao Za Zhi. 2021;46(1):15-23. doi: 10.19540/j.cnki.cjcmm.20201012.601. [Chinese].
33. Sorrenti V, Raffaele M, Vanella L, Acquaviva R, Salerno L, Pittalà V, et al. Protective effects of caffeic acid phenethyl ester (CAPE) and novel cape analogue as inducers of heme oxygenase-1 in streptozotocin-induced type 1 diabetic rats. Int J Mol Sci. 2019;20(10):2441. doi: 10.3390/ijms20102441.
34. Wang X, Jiang Y, Zhou P, Lin L, Yang Y, Yang Q, et al. Effective natural inhibitors targeting granzyme B in rheumatoid arthritis by computational study. Front Med (Lausanne). 2022;9:1052792. doi: 10.3389/fmed.2022.1052792.